This is a preprint, the final version is subject to change, of the American Mineralogist (MSA)
Cite as Authors (Year) Title. American Mineralogist, in press.
(DOI will not work until issue is live.) DOI: http://dx.doi.org/10.2138/am-2016-5577

Revision 1.

Association of cumulus apatite with compositionally unusual olivine and plagioclase in the Taihe Fe-Ti oxide ore-bearing layered mafic-ultramafic intrusion: Petrogenetic significance and implications for ore genesis

Zhong-Jie Bai[a], Hong Zhong[a]*, Chusi Li[b], Wei-Guang Zhu[a], Wen-Jun Hu[a, c]

[a] State Key Laboratory of Ore Deposit Geochemistry, Institute of Geochemistry, Chinese Academy of Sciences, Guiyang 550081, China
[b] Department of Geological Sciences, Indiana University, Indiana 47405, USA
[c] University of Chinese Academy of Sciences, Beijing 100049, China

* Corresponding author. Tel.:+86 851 8589 1820;
Fax: +86 851 8589 1664.
E-mail: zhonghong@vip.gyig.ac.cn (H. Zhong).

Abstract

In many large layered mafic-ultramafic intrusions worldwide cumulus apatite commonly occurs in the highly fractionated, Fe-Ti oxide-rich lithological units at the top of the intrusions and the associated plagioclase and olivine, if present, have An content <50 mol% and Fo content <40 mol%. These are not true for several Fe-Ti oxide ore-bearing mafic-mafic intrusions in the Emeishan large igneous province, SW China. A good example is the Taihe intrusion, which is described in this paper. In this intrusion the associated olivine and plagioclase are significantly more primitive, containing 69 mol% Fo and 59 mol% An, respectively. MELTS simulation reveals that such unusual association is the result of previous cotectic crystallization of Fe–Ti oxides with silicate minerals during magma evolution under oxidizing condition close to that of nickel–nickel oxide buffer. Supports for this new model include the observed upward decrease in plagioclase An contents coupled by lack of significant change in original olivine Fo contents in the Fe-Ti oxide ore-bearing sequence below the apatite-rich horizon, which is in turn supported by the facts that Fe-Ti oxide crystallization has a counter effect on MgO/FeO but no effect on CaO/Na_2O in the residual magma and that the addition of Fe-Ti oxides in the cumulus assemblage expedites the arrival of apatite on the liquidus. Our new findings support the interpretation that the oxide ores in the Taihe intrusion formed by gravitational accumulation of Fe–Ti oxides crystallizing from a basaltic magma, not a Fe-Ti-P-rich immiscible liquid segregated from such magma.

Key words: Cumulus apatite; Fe-Ti oxides; Olivine; Plagioclase; Magma differentiation; Layered intrusion

This is a preprint, the final version is subject to change, of the American Mineralogist (MSA)
Cite as Authors (Year) Title. American Mineralogist, in press.
(DOI will not work until issue is live.) DOI: http://dx.doi.org/10.2138/am-2016-5577

Introduction

Phosphorus is an incompatible element during fractional crystallization of silicate minerals from basaltic magma. The content of phosphorus in apatite-saturated magma is mainly a function of temperature and SiO_2 concentration in the magma but almost insensitive to pressure according to the experiments of Watson (1979) and Tollari et al. (2006, 2008). These experiments show that the maximum solubility of phosphorus at apatite saturation in basaltic magma increases with temperature and decreases with SiO_2 content. The content of SiO_2 in a basaltic magma commonly increases during the crystallization of silicate minerals plus minor spinel from the magma on cooling. As a result, fractional crystallization not only increases the abundance of phosphorus in the residual liquid but also decreases the maximum solubility of phosphorus in the magma, thereby inducing apatite crystallization eventually. In natural basaltic systems this takes place most commonly when the residual liquid is also saturated with Fe–Ti oxides. The best examples worldwide are the Bushveld, Skaergaard, Kiglapait and Sonju Lake layered mafic-ultramafic intrusions in which the cumulus apatite horizons also contain abundant Fe-Ti oxides. The apatite-oxide layers occur at the top of these intrusions and the associated plagioclase and olivine have An content <50 mol% and Fo content <40 mol%, which are thought to have formed from highly evolved basaltic-andesitic melt after extensive fractional crystallization (Morse, 1979; McBirney, 1996; Park et al., 2004; Tegner et al., 2006). An exception has been found in several mafic-ultramafic layered intrusions of the Emeishan large igneous province in SW China, such as the Panzhihua (Zhou et al., 2005; Pang et al., 2008a, b, 2009; Song et al., 2013), Hongge (Bai et al., 2012, 2014; Luan et al., 2014) and Taihe (Shellnutt et al., 2011; Hou et al., 2012; She et al., 2014) intrusions. In these intrusions cumulus apatite horizons occur above several massive Fe–Ti oxide layers (Fig. 1). In addition, the associated olivine and plagioclase are much more

primitive in these intrusions than those occur elsewhere in the world (Table 1 and Fig. 2). The reasons for these differences and their implications will be discussed in this paper.

Geological setting

The Emeishan large igneous province is composed of picrites, flood basalts, rhyolitic/trachytic volcanic rocks, mafic–ultramafic layered intrusions, granites, and syenites. It is widely believed to be related to mantle plume activity located in the western margin of the Yangtze Craton, SW China (Chung and Jahn, 1995). Some of the mafic-ultramafic layered intrusions in the Emeishan large igneous province host world-class Fe-Ti oxide ore deposits. They are partially exposed in the inner zone of the province in the Panzhihua–Xichang (Pan–Xi) region where a series of NS–trending major faults occur. The most important Fe–Ti oxide ore-bearing intrusions in the region include the Panzhihua (Zhou et al., 2005; Pang et al., 2008a, b, 2009; Song et al., 2013), Hongge (Bai et al., 2012, 2014; Luan et al., 2014), Taihe (Shellnutt et al., 2011; Hou et al., 2012; She et al., 2014), Baima (Zhang et al., 2012; Liu et al., 2014), and Xinjie (Zhong et al., 2011a) intrusions. These five intrusions together contain a total ore reserve of ~7,209 Mt Fe_2O_3, ~559 Mt TiO_2, and ~17.4 Mt V_2O_3 with grades of 27 wt % FeO, 10.6 wt % TiO_2, and 0.24 wt % V_2O_3 (Ma et al., 2003; Zhong et al., 2005). Each of these deposits contains several massive Fe–Ti oxide (magnetite + ilmenite) layers, mostly in the lower parts of the intrusions. The thicknesses of the oxide layers vary from several meters to nearly one hundred meters (Fig. 1). An apatite-rich horizon (up to 10 wt% apatite) occurs in these intrusions above the massive oxide layers.

Lithology of the Taihe intrusion

The Taihe layered mafic intrusion is located to the west of the Xichang city. It is 4-km long and 3.5-km wide on the surface. Zircon from this intrusion yields a U-Pb age of 258.8 ± 2.3 Ma (Zhong et al., 2011b), similar to the zircon U-Pb age (259.6 ± 5.9 Ma) of the associated flood basalts in this region (Fan et al., 2008; Lai et al., 2012). The lithological structure of the Taihe intrusion was described in details by many researchers (e.g., Li et al., 1981; Shellnutt et al., 2011; Zhong et al., 2011b; Hou et al., 2012; She et al., 2014). It was originally divided into three zones by Li et al. (1981): a lower zone which is predominantly composed of melanogabbros, a middle zone which is composed of oxide melanogabbros and massive oxide layers, and an upper zone which is mainly composed of leucogabbros. In this study we divide it into only two zones so that each zone contains cumulus apatite at the top (Fig. 1). The lower zone is ~260-m thick. It is composed of oxide gabbro, massive oxide ores and apatite-bearing gabbro from the bottom to the top. The oxide gabbro in this zone is composed of cumulus clinopyroxene (25–40 vol%), plagioclase (25–45 vol%), magnetite (10–35 vol%), ilmenite (5-10 vol%) and minor olivine and hornblende (<5 vol%) (Fig. 3a). The associated massive Fe-Ti-V oxide layers, which account for the majority of the ore resources in the intrusion, contain >80 vol% oxides (magnetite and ilmenite) and <20 vol% silicate minerals (clinopyroxene, plagioclase and olivine). Cumulus apatite occurs in the uppermost 50 m of this zone to form an apatite-rich gabbro containing 5-10 vol% apatite, 20-30 vol% plagioclase, 30-40 vol% clinopyroxene, 20-30 vol% magnetite, 5-10 vol% ilmenite and minor olivine and hornblende (<5 vol%) (Fig. 3b). The upper zone of the intrusion is 1000-m thick (Fig. 1). It consists of a thin oxide gabbro layer at the bottom and a thick apatite-rich gabbro layer at the top. The modal compositions of the gabbros in the lower and upper zones are generally similar but no massive Fe-Ti oxide layer is present in the upper zone.

Analytical methods

The samples used in this study were collected from the lower zone of the Taihe intrusion. The chemical compositions of olivine, plagioclase were determined by wavelength-dispersive X-ray analysis using an EPMA-1600 electron microprobe at the State Key Laboratory of Ore Deposit Geochemistry, Institute of Geochemistry, Chinese Academy of Sciences, Guiyang, China. The analytical conditions were 10 nA beam current, 25 kV acceleration voltage and 10-μm beam size. Both natural and synthetic standards were used for calibration. The analytical uncertainty is ~2%.

Whole-rock major element compositions of the samples were determined using X-ray fluorescence spectrometry by the ALS Laboratory Group in Guangzhou, China. The analytical uncertainty is better than 5%. Trace elements of whole rocks were analyzed using a Perkin-Elmer Sciex ELAN DRC–e Quadrupole Inductively Coupled Plasma Mass Spectrometer (Q–ICP–MS) at the State Key Laboratory of Ore Deposit Geochemistry, Institute of Geochemistry, Chinese Academy of Sciences (SKLODG, IGCAS). The analytical precision for trace elements is generally better than 10% relative standard deviation.

Results

The average plagioclase, olivine compositions and whole-rock FeO^T contents in the lower zone of the Taihe intrusion are listed in Tables 2, 3 and supplementary material 1. The An contents of plagioclase and the Fo contents of olivine in this zone vary from 57 to 79 mol% and from 66 to 80 mol%, respectively (Table 3). The Fo content of olivine and the An content of plagioclase in the lowest layer of apatite-rich rocks in the Taihe intrusion are 69 mol% and 59 mol%, respectively. These values are similar to those for the Panzhihua layered intrusion in the Emeishan large igneous province but are

significantly higher than those for other mafic-ultramafic layered intrusions elsewhere in the world such as Bushveld in South Africa, Skaergaard in East Greenland, Sonju Lake in Minnesota, USA, and Kiglapait and Newark Island in Labrador, Canada (Table 1, Fig. 2).

The Fo content of olivine in intrusive rocks may have been modified by re-equilibration with trapped liquids (Barnes, 1986). However, the content of nearly perfectly incompatible trace elements such as U (<0.1ppm) and Th (<0.5ppm) in all the olivine-bearing gabbro of the lower zone is extremely low compared with the coeval Emeishan high-Ti basalts (1.2 ppm of U and 5.1 ppm of Th in average; GEOROC), indicating the amounts of trapped liquid in the lower zone are estimated to be <10 wt.%. This means that the trapped liquid shifts for olivine Fo content from the lower zone are similar and small; probably less than 2% based on the calculations of Barnes (1986). The samples from the lower zone of the Taihe intrusion collectively show a positive correlation between olivine Fo content and whole-rock FeO^T abundance (Fig. 4), of which the FeO^T is proxy for the amount of Fe-Ti oxides in the sample. This indicates that the composition of olivine in this zone was modified by the subsolidus Fe–Mg exchange reaction between olivine and coexisting Fe–Ti oxides on cooling, a process that is common for oxide-rich rocks in layered intrusions such as Kiglapait (Morse, 1980). The observed correlation in the Taihe samples reveals that an increase of 1 wt% FeO^T in whole rock resulted in an increase of 0.34 mol% Fo in olivine. We have used this relationship to correct the effect of the subsolidus re-equilibration on the composition of olivine in the samples. The corrected Fo contents of olivine in the samples are shown in Fig. 5a. Except one sample, the corrected Fo contents of olivine in the lower zone of the Taihe intrusion are close to 66 mol% and don't show any systematic variation with depth (Fig. 5a). In contrast, the An contents of plagioclase in this zone generally decease upward from 71 mol% at the base to 57 mol% at the top (Fig. 5b).

This is a preprint, the final version is subject to change, of the American Mineralogist (MSA)
Cite as Authors (Year) Title. American Mineralogist, in press.
(DOI will not work until issue is live.) DOI: http://dx.doi.org/10.2138/am-2016-5577

Modeling and discussion

The consequence of early Fe-Ti oxide crystallization

Magma saturation in apatite is mainly controlled by temperature and the concentrations of P_2O_5 and SiO_2 (Watson, 1979; Tollari et al., 2006). The results from these experimental studies show that the P_2O_5 content at apatite saturation in magma, or the maximum solubility of P_2O_5, is negatively correlated with SiO_2 content and positively correlated with temperature, and that the initial contents of P_2O_5 in natural basalts are several times below the maximum solubility. As a result, extensive fractional crystallization of silicate minerals such as olivine, pyroxene and plagioclase on cooling, which increases P_2O_5 and SiO_2 concentrations in the residual liquid, is required to induce apatite saturation in basaltic magma. This explains why cumulus apatite occurs in the highly evolved lithological units of many large mafic-ultramafic layered intrusions in the world such as the Bushveld, Skaergaard, Sonju Lake, Kiglapait and Newark Island intrusions (Morse, 1979; McBirney, 1996; Park et al., 2004; Tegner et al., 2006). Extensive fractional crystallization as the main reason for the arrival of cumulus apatite in these magmatic systems are clearly indicated by low An contents (34-48 mol%) of plagioclase as well as low Fo contents of olivine (16-39 mol%) in the cumulus apatite-bearing horizons of these intrusions (Fig. 2). By comparison, olivine and plagioclase in the cumulus apatite-bearing lithological units of the Taihe and Panzhihua mafic-ultramafic layered intrusions in the Emeishan large igneous province are much more primitive, containing 65-69 mol% Fo and 53-59 mol% An, respectively (Table 1 and Fig. 2).

What cause the differences described above? We can identify two alternative possibilities: (1) unusually high initial P_2O_5 content in the Panzhihua-Taihe parent magmas or (2) early removal of

Fe-Ti oxides from the parent magmas of these intrusions. It is very difficult to know the initial contents of P_2O_5 in the parental magmas of these intrusions but the contents of P_2O_5 in the coeval flood basalts are normal as compared to continental flood basalts elsewhere in the world (Fig. 6).

How does the second possibility work? The Fo content of olivine and An content of plagioclase decrease progressively during fractional crystallization of silicate minerals without Fe-Ti oxides. Addition of Fe-Ti oxide crystallization with silicate minerals has an opposite effect on the Fo content of olivine but no effect on the An content of plagioclase. Removal of silicate minerals and Fe-Ti oxides from magma also contributes to P_2O_5 enrichment in the residual liquid, thereby expediting magma saturation in apatite. The combined effect of early Fe-Ti oxide crystallization with silicate minerals is that apatite will appear on the liquidus with more primitive olivine and plagioclase than otherwise.

Evidence from MELTS simulation

The ratio of Fe_2O_3/FeO in basaltic magma is a function of oxidation state. A more oxidizing condition will speed up magma saturation in Fe-Ti oxides (Toplis and Carroll, 1995). We have evaluated such an effect using the pMETLS program of (Ghiorso et al., 2002) under two different oxidation states, a relatively reducing condition equivalent to FMQ–1 (FMQ, fayalite–magnetite–quartz buffer) and a relatively oxidizing condition equivalent to NNO (nickel–nickel oxide buffer). As the mantle-derived magma was trapped in the middle crust before emplaced into the upper crust to form the Fe-Ti-V-oxide-bearing intrusions of the ELIP (Tao et al., 2015), in our two-stage modeling of fractionation in the deep-seated (middle crust) and shallower magma chambers (pluton), the pressures were assumed at 7 kbar and 3 kbar. The composition of melt

inclusion (M8-62, supplementary material 2) hosted in olivine containing Fo92 (Kamenetsky et al., 2012) was used to represent the initial magma composition because it has the highest MgO content in the most forsteritic olivine of the Emeishan high-Ti picrites in the Pan-Xi area and thus represents the most primitive magma of these related intrusions. The initial content of P_2O_5 in the magma was assumed to be 0.25 wt%, which is the average P_2O_5 content of the high-Ti picrites in the Emeishan large igneous province (Kamenetsky et al., 2012). The H_2O content was set to 0.6 wt% as considerable hornblende was present. The timing of magma saturation in apatite during fractional crystallization is inferred from a comparison with the temperature-SiO_2 relation for apatite-saturated magma determined experimentally by Green and Watson (1982). Under oxidizing condition, apatite appears on the liquidus close to 1045°C together with olivine and plagioclase having Fo_{76} and An_{55}, respectively (supplementary material 2). The inferred composition is similar to the composition of olivine and plagioclase (Fo_{65-72} and An_{53-59}, Table 1) at the onset of apatite saturation in these intrusions. In contrast, under reducing condition, apatite appears on the liquidus at lower temperature together with more evolved olivine composition of Fo_{54}. Moreover, the modeling TiO_2 content of magnetite, which is negatively correlated with fO_2 (Buddington and Lindsley, 1964), is about 16.7 wt% at NNO (supplementary material 2), resemble to the primary magnetite compositions (16.5 wt% of TiO_2, Pang et al., 2008b). It should be pointed out that the oxidizing condition used in our model is within the stability field of sulfide (Jugo et al., 2005). Thus, the results are applicable to the Panzhihua-Taihe intrusions where magmatic sulfides are present (Pang et al., 2008a, She et al., 2014).

Evidence from mineral composition

Crystallization of Fe-Ti oxides before apatite saturation in the Panzhihua-Taihe magmatic systems

238 is clearly indicated by the occurrence of massive oxide layers below apatite-rich horizons in these
239 intrusions (Fig. 1). Our modeling results (Fig. 6b) clearly show that when Fe-Ti oxides join silicate
240 minerals on the liquidus at early stage on cooling at relatively oxidizing condition, the Mg number
241 [Mg# = (100MgO/FeO, molar)] of liquid no longer decreases with further fractional crystallization.
242 This explains why the Fo content of olivine in the Taihe intrusion remains rather constant with depth
243 and higher at apatite saturation than those occur elsewhere in the world (Fig. 5a). Olivine is a Fe-Mg
244 silicate solid solution. Its Fo content is related to the Mg number of the liquid. In basaltic system the
245 Fe-Mg exchange coefficient or K_D $[(FeO/MgO)^{olivine}/(FeO/MgO)^{liquid}]$ is close to 0.3, largely
246 independent of temperature and composition (Roeder and Emslie, 1970). In Fig. 5a, the olivine
247 composition is clearly buffered to a single value upwards in the stratigraphy, and this happens because
248 the oxygen fugacity is roughly constant in the presence of the magnetite layers, thereby the Mg# of the
249 silicate liquid is almost unchanged.

250 The average An content of coexisting plagioclase continues to decrease upward after the arrival of
251 cumulus Fe-Ti oxide (Fig. 5b), because the crystallization of Fe-Ti oxides does not affect the Ca/Na
252 ratio which controls plagioclase composition. The massive Fe-Ti oxide ore layers in the Taihe
253 intrusion contain plagioclase with average An content up to 70 mol% (Fig. 5b), which is ~10-20 mol%
254 higher than this type of plagioclase in other large layered intrusions elsewhere in the world such as
255 Bushveld and Skaergaard intrusions (McBirney, 1996; Tegner et al., 2006). This provides another line
256 of evidence that the parental magmas of the Panzhihua-Taihe Fe-Ti oxide ore deposits are more
257 primitive than the same type of deposit elsewhere in the world. Abundant Fe-Ti oxide crystallization at
258 early stage would significantly increase the SiO_2 content of the residual magma because of negligible
259 SiO_2 content in Fe-Ti oxide, which in turn speeds up apatite saturation in the residual liquid. As shown

in Fig. 6a, the SiO_2 content of the magma increases more quickly with magma differentiation after Fe-Ti oxide saturation at relatively oxidizing condition than at relatively reducing condition. This explains why the An content of plagioclase at apatite saturation is higher than those elsewhere in the world (Fig. 2; Table 1).

Implications for the genesis of Panzhihua-type Fe–Ti oxide deposit

The Fe–Ti oxide ores in the Panzhihua-type deposit (Pang et al., 2008a, Bai et al., 2012; She et al., 2014) such as Taihe occur as concordant layers below apatite-rich horizons in the mafic-ultramafic layered intrusions of the Emeishan large igneous province. The origin of the Panzhihua-type Fe-Ti oxide ores is hotly debated. Some researchers proposed that the oxide ores formed by concentration of immiscible Fe–Ti-enriched liquid segregated from ferrobasaltic magma (Zhou et al., 2005; Liu et al., 2014). Other researchers believed that they formed by accumulation of Fe–Ti oxides crystallizing from basaltic magma under oxidizing condition (Ganino et al., 2008; Pang et al., 2008a, b; Bai et al., 2012; Howarth and Prevec, 2013; Song et al., 2013). The immiscibility model is not supported by experimental results. Under geologically reasonable conditions, silicate liquid immiscibility only occurs in a highly evolved basaltic magma which crystallizes olivine containing Fo <43 mol% and plagioclase containing An <60 mol% (Charlier and Grove, 2012). The Fe–Ti–rich immiscible melt is also enriched in P_2O_5 and contains <32 wt% FeO^{Total}, significantly different from the compositions of typical Panzhihua-type oxide ores. The immiscible Fe-Ti-P-rich melt also has very low Mg# [Mg#<21, Mg# = (100MgO/FeO, molar)] and contains significant amounts of SiO_2 (33-52 wt%), CaO (8-11 wt%) and Al_2O_3 (2-10 wt%) (Charlier and Grove, 2012). On cooling, such melt will form an ilmenite–magnetite–rich rock containing significant amounts of apatite, low-An plagioclase and

low-Mg# olivine or clinopyroxene (Charlier et al., 2015). Physical separation between denser crystals (Fe-Ti oxides and apatite) and lighter crystals (silicate minerals) may occur in a dynamic system, forming a Fe-Ti oxide-apatite concentrate. Contrary to the experimental predictions, cumulus apatite horizons in the Panzhihua-type deposit always occur above the Fe-Ti oxide ore layers (Fig. 1). In addition, olivine and plagioclase associated with the oxide ores are significantly more primitive than experimental results. The fractional crystallization model can well explain these features plus other important features such as the upward decrease in plagioclase An contents coupled with a rather constant olivine Fo contents in the oxide ore-bearing sequence. According to this model, the massive Fe-Ti oxide ores in the Panzhihua-type Fe-Ti oxide deposit is thought to have formed by crystal fractionation in a dynamic magmatic system.

CONCLUSIONS

Olivine and plagioclase associated with cumulus apatite in the Taihe mafic-ultramafic layered intrusion of the Emeishan large igneous province are more primitive than those in many well-known large layered mafic-ultramafic intrusions elsewhere in the world. The Fe-Ti oxide ore-bearing sequence below the cumulus apatite horizon in the Taihe intrusion shows an upward decrease in plagioclase An content coupled by rather constant olivine Fo content. These features can all be explained by cotectic crystallization of Fe-Ti oxides with the silicate minerals on cooling. MELTS simulation indicates that such cotectic crystallization will prevail under an oxidizing condition close to the NNO buffer and that the addition of Fe-Ti oxides in the crystallizing assemblage will speed up apatite saturation in the residual liquid. The results from this study support the interpretation that the oxide ores in the Taihe intrusion formed by gravitational accumulation of Fe–Ti oxides crystallizing

304 from a basaltic magma, not a Fe-Ti-P-rich immiscible liquid segregated from such magma.

305

306 **ACKNOWLEDGMENTS**

307 We thank WQ Zheng in the State Key Laboratory of Ore Deposit Geochemistry for the assistance
308 in EMPA analysis. The helpful and constructive reviews by Professors S. A. Morse and D. H. Lindsley,
309 along with those of the Editor, Julie Roberge, are gratefully acknowledged. This study was jointly
310 supported by the National Basic Research Program of China (2014CB440903), the National Natural
311 Science Foundation of China (41203040, 41473048, 41425011), West Light Foundation of the Chinese
312 Academy of Sciences, and Guizhou Provincial Natural Science Foundation (2294 of Y2013).

313

314 **REFERENCES CITED**

315 Bai, Z.J., Zhong, H., Li, C., Zhu, W.G., He, D.F., and Qi, L. (2014) Contrasting parental magma
316 compositions for the Hongge and Panzhihua magmatic Fe-Ti-V oxide deposits, Emeishan
317 Large Igneous Province, SW China. Economic Geology, 109, 1763-1785.
318 Bai, Z.J., Zhong, H., Naldrett, A.J., Zhu, W.G., and Xu, G.W. (2012) Whole-Rock and Mineral
319 Composition Constraints on the Genesis of the Giant Hongge Fe–Ti–V Oxide Deposit in the
320 Emeishan Large Igneous Province, Southwest China. Economic Geology, 107, 507-524.
321 Barnes, S. J. (1986) The effect of trapped liquid crystallization on cumulus mineral compositions in
322 layered intrusions. Contributions to Mineralogy and Petrology, 93, 524-531.
323 Buddington, A.F. and Lindsley, D.H. (1964) Iron-Titanium Oxide Minerals and Synthetic Equivalents.
324 Journal of Petrology, 5, 310-357.
325 Charlier, B. and Grove, T. (2012) Experiments on liquid immiscibility along tholeiitic liquid lines of

326 descent. Contributions to Mineralogy and Petrology, 164, 27-44.

327 Charlier, B., Namur, O., Bolle, O., Latypov, R., and Duchesne, J-C. (2015) Fe–Ti–V–P ore deposits
328 associated with Proterozoic massif-type anorthosites and related rocks. Earth-science Reviews,
329 141, 56-81.

330 Chung, S-L. and Jahn, B-m. (1995) Plume-lithosphere interaction in generation of the Emeishan flood
331 basalts at the Permian-Triassic boundary. Geology, 23, 889-892.

332 Fan, W.M., Zhang, C.H., Wang, Y.J., Guo, F., and Peng, T.P. (2008) Geochronology and geochemistry
333 of Permian basalts in western Guangxi Province, Southwest China: Evidence for
334 plume-lithosphere interaction. Lithos, 102, 218-236.

335 Ganino, C., Arndt, N., Zhou, M-F., Gaillard, F., and Chauvel, C. (2008) Interaction of magma with
336 sedimentary wall rock and magnetite ore genesis in the Panzhihua mafic intrusion, SW China.
337 Mineralium Deposita, 43, 677-694.

338 Ghiorso, M.S., Hirschmann, M.M., Reiner, P.W., and Kress, V.C. (2002) The pMELTS: a revision of
339 MELTS for improved calculation of phase relations and major element partitioning related to
340 partial melting of the mantle to 3 GPa. Geochemistry, Geophysics, Geosystems, 3, 1-35.

341 Green, T.H. and Watson, E.B. (1982) Crystallization of apatite in natural magmas under high pressure,
342 hydrous conditions, with particular reference to ‘Orogenic’ rock series. Contributions to
343 Mineralogy and Petrology, 79, 96-105.

344 Hou, T., Zhang, Z., Encarnacion, J., and Santosh, M. (2012) Petrogenesis and metallogenesis of the
345 Taihe gabbroic intrusion associated with Fe–Ti-oxide ores in the Panxi district, Emeishan
346 Large Igneous Province, southwest China. Ore Geology Reviews, 49, 109-127 .

347 Howarth, G.H., and Prevec, S.A. (2013) Trace element, PGE, and Sr–Nd isotope geochemistry of the

Panzhihua mafic layered intrusion, SW China: Constraints on ore-forming processes and evolution of parent magma at depth in a plumbing-system. Geochimica et Cosmochimica Acta, 120, 459-478.

Jugo, P.J., Luth, R.W., and Richards, J.P. (2005) Experimental data on the speciation of sulfur as a function of oxygen fugacity in basaltic melts. Geochimica et Cosmochimica Acta, 69, 497–503.

Kamenetsky, V.S., Chung, S-L., Kamenetsky, M.B., and Kuzmin, D.V. (2012) Picrites from the Emeishan Large Igneous Province, SW China: a Compositional Continuum in Primitive Magmas and their Respective Mantle Sources. Journal of Petrology, 53, 2095-2113 .

Lai, S.C., Qin, J.F., Li, Y.F., Li, S.Z., and Santosh, M. (2012) Permian high Ti/Y basalts from the eastern part of the Emeishan Large Igneous Province, southwestern China: Petrogenesis and tectonic implications. Journal of Asian Earth Sciences, 47, 216-230.

Li, D.H., Chen, Z.X., and Han, Z.W. (1981) RythmicRhythmic layers and petrological characteristics of Taihe layered intrusion. J.Chengdu Univ. Technol. (Science & Technology Edition), 3, 9–21 (in Chinese).

Liu, D., Shen, F.K., and Zhang, G.Z. (1985) Layered intrusions of the Panxi area, Sichuan province, in Zhang, Y.X., ed., Corpus of the Panxi paleorift studies in China. Geological Press, pp 85–118 (in Chinese).

Liu, P.P., Zhou, M-F., Chen, W.T., Boone, M., and Cnudde, V. (2014) Using Multiphase Solid Inclusions to Constrain the Origin of the Baima Fe–Ti–(V) Oxide Deposit, SW China. Journal of Petrology, 55, 951-976.

Luan, Y., Song, X.Y., Chen, L.M., Zheng, W.Q., Zhang, X.Q., Yu, S.Y., She, Y.W., Tian, X.L., and Ran,

Q.Y. (2014) Key factors controlling the accumulation of the Fe–Ti oxides in the Hongge layered intrusion in the Emeishan Large Igneous Province, SW China. Ore Geology Reviews, 57, 518-538.

Ma, Y., Ji, X.T., Li, J.C., Huang, M., and Kan, Z.Z. (2003) Mineral resources of the Panzhihua region. Chengdu, Sichuan Science and Technology Press, 275 p. (in Chinese).

McBirney, A.R., 1996. The Skaergaard Intrusion, in Cawthorn, R.G., ed., Layered intrusions. New York, Elsevier, pp 147–180.

Morse, S.A. (1979) Kiglapait Geochemistry I: Systematics, Sampling, and Density. Journal of Petrology, 20, 555-590.

Morse, S.A. (1980) Kiglapait Mineralogy II: Fe-Ti Oxide Minerals and the Activities of Oxygen and Silica. Journal of Petrology, 21, 685-719.

Pang, K-N., Li, C., Zhou, M-F., and Ripley, E. (2008a) Abundant Fe–Ti oxide inclusions in olivine from the Panzhihua and Hongge layered intrusions, SW China: evidence for early saturation of Fe–Ti oxides in ferrobasaltic magma. Contributions to Mineralogy and Petrology, 156, 307-321.

Pang, K-N., Li, C., Zhou, M-F., Ripley, and E.M. (2009) Mineral compositional constraints on petrogenesis and oxide ore genesis of the late Permian Panzhihua layered gabbroic intrusion, SW China. Lithos, 110, 199-214.

Pang, K-N., Zhou, M-F., Lindsley, D., Zhao, D.G., and Malpas, J. (2008b) Origin of Fe-Ti Oxide Ores in Mafic Intrusions: Evidence from the Panzhihua Intrusion, SW China. Journal of Petrology, 49, 295-313 .

Park, Y-R., Ripley, E.M., Miller, J.D., Li, C., Mariga, J., and Shafer, P. (2004) Stable Isotopic

392 Constraints on Fluid-Rock Interaction and Cu-PGE-S Redistribution in the Sonju Lake
393 Intrusion, Minnesota. Economic Geology, 99, 325-338.
394 Roeder, P.L., and Emslie, R.F. (1970) Olivine-liquid equilibrium. Contributions to Mineralogy and
395 Petrology, 29, 275-289.
396 She, Y.W., Yu, S.Y., Song, X.Y., Chen, L.M., Zheng, W.Q., and Luan, Y. (2014) The formation of
397 P-rich Fe–Ti oxide ore layers in the Taihe layered intrusion, SW China: Implications for
398 magma-plumbing system process. Ore Geology Reviews, 57, 539-559.
399 Shellnutt, J.G., Wang, K-L., Zellmer, G.F., Iizuka, Y., Jahn, B-M., Pang, K-N., Qi, L., and Zhou, M-F.
400 (2011) Three Fe-Ti oxide ore-bearing gabbro-granitoid complexes in the Panxi region of the
401 Permian Emeishan large igneous province, SW China. American Journal of Science, 311,
402 773-812.
403 Song, X.Y., Qi, H.W., Hu, R.Z., Chen, L.M., Yu, S.Y., and Zhang, J.F. (2013) Formation of thick
404 stratiform Fe-Ti oxide layers in layered intrusion and frequent replenishment of fractionated
405 mafic magma: Evidence from the Panzhihua intrusion, SW China. Geochemistry, Geophysics,
406 Geosystems, 14, 712-732.
407 Tao, Y., Putirka, K., Hu, R.Z., and Li, C. (2015) The magma plumbing system of the Emeishan large
408 igneous province and its role in basaltic magma differentiation in a continental setting.
409 American Mineralogist, 100, 2509-2517.
410 Tegner, C., Cawthorn, R.G., and Kruger, F.J. (2006) Cyclicity in the Main and Upper Zones of the
411 Bushveld Complex, South Africa: Crystallization from a Zoned Magma Sheet. Journal of
412 Petrology, 47, 2257-2279.
413 Tollari, N., Baker, D., and Barnes, S.J. (2008) Experimental effects of pressure and fluorine on apatite

saturation in mafic magmas, with reference to layered intrusions and massif anorthosites. Contributions To Mineralogy and Petrology, 156, 161-175.

Tollari, N., Toplis, M.J., and Barnes, S.J. (2006) Predicting phosphate saturation in silicate magmas: An experimental study of the effects of melt composition and temperature. Geochimica et Cosmochimica Acta, 70, 1518-1536.

Toplis, M.J., and Carroll, M.R. (1995) An Experimental Study of the Influence of Oxygen Fugacity on Fe-Ti Oxide Stability, Phase Relations, and Mineral--Melt Equilibria in Ferro-Basaltic Systems. Journal of Petrology, 36, 1137-1170.

Watson, E.B. (1979) Apatite saturation in basic to intermediate magmas. Geophysical Research Letters, 6, 937-940.

Wiebe, R.A., and Snyder, D. (1993) Slow, dense replenishments of a basic magma chamber: the layered series of the Newark Island layered intrusion, Nain, Labrador. Contributions to Mineralogy and Petrology, 113, 59-72.

Zhang, X.Q., Song, X.Y., Chen, L.M., Xie, W., Yu, S.Y., Zheng, W.Q., Deng, Y.F., Zhang, J.F., and Gui, S.G. (2012) Fractional crystallization and the formation of thick Fe–Ti–V oxide layers in the Baima layered intrusion, SW China. Ore Geology Reviews, 49, 96-108.

Zhong, H., Hu, R.Z., Wilson, A., and Zhu, W.G. (2005) Review of the Link between the Hongge Layered Intrusion and Emeishan Flood Basalts, Southwest China. International Geology Review, 47, 971-985.

Zhong, H., Campbell, I.H., Zhu, W.G., Allen, C.M., Hu, R.Z., Xie, L.W., and He, D.F. (2011b) Timing and source constraints on the relationship between mafic and felsic intrusions in the Emeishan large igneous province. Geochimica et Cosmochimica Acta, 75, 1374-1395.

Zhong, H., Qi, L., Hu, R.Z., Zhou, M.F., Gou, T.Z., Zhu, W.G., Liu, B.G., and Chu, Z.Y. (2011a) Rhenium-osmium isotope and platinum-group elements in the Xinjie layered intrusion, SW China: Implications for source mantle composition, mantle evolution, PGE fractionation and mineralization. Geochimica et Cosmochimica Acta, 75, 1621-1641.

Zhou, M-F., Robinson, P.T., Lesher, C.M., Keays, R.R., Zhang, C.J., and Malpas, J. (2005) Geochemistry, Petrogenesis and Metallogenesis of the Panzhihua Gabbroic Layered Intrusion and Associated Fe-Ti-V Oxide Deposits, Sichuan Province, SW China. Journal of Petrology, 46, 2253-2280.

Figure captions:

Fig. 1. Simplified stratigraphy of the Panzhihua, Hongge and Taihe Fe-Ti oxide ore-bearing mafic-ultramafic layered intrusions, showing the locations of Fe–Ti oxide ore layers and cumulus apatite horizons.

Fig. 2. Compositions of olivine and plagioclase associated with cumulus apatite in some layered mafic-ultramafic intrusions in the world. Data are from Table 1.

Fig. 3. Photomicrographs showing (a) cumulus olivine-Fe-Ti oxide assemblage in the olivine-bearing

458 gabbro and (b) cumulus apatite-olivine assemblage in the apatite and olivine-bearing gabbro in the
459 Taihe intrusion. Ol= olivine, Cpx= clinopyroxene, Pl= plagioclase. Ap= apatite.
460
461 Fig. 4. Correlation between olivine Fo contents and whole-rock FeO^{Total} concentrations in the Taihe
462 intrusion, showing that 1 wt% FeO^{Total} increase in whole rocks corresponds to 0.34 mol% Fo increase
463 in olivine.
464
465 Fig. 5. Stratigraphic variations of adjusted olivine Fo contents (a) and observed plagioclase An
466 contents (b) in the Taihe intrusion. See text for an explanation for the adjustment.
467
468 Fig. 6. Results of fractional crystallization of picritic magma simulated using the MELTS program
469 (Ghiorso and Sack, 1995). The composition of melt inclusion (M8-62) hosted in olivine of Fo92
470 (Kamenetsky et al., 2012) is used to represent the initial composition of the magma. The assumed
471 initial P_2O_5 content in the magma is similar to the upper limit of picrites from the Emeishan large
472 igneous province. The compositions of picrites and high-Ti basalts are from a petrogolical database
473 (http://georoc.mpch-mainz.gwdg.de/georoc). The dashed lines are apatite saturation curves from Green
474 and Watson (1982).

This is a preprint, the final version is subject to change, of the American Mineralogist (MSA)
Cite as Authors (Year) Title. American Mineralogist, in press.
(DOI will not work until issue is live.) DOI: http://dx.doi.org/10.2138/am-2016-5577

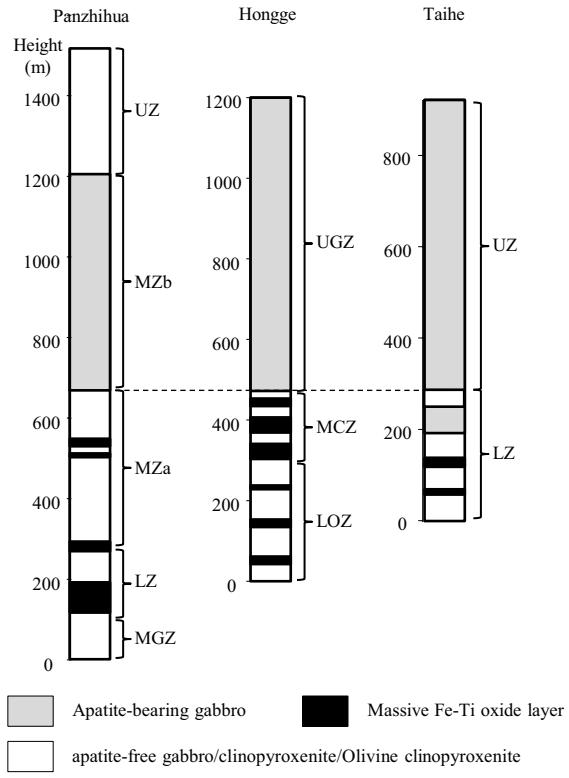

Fig. 1

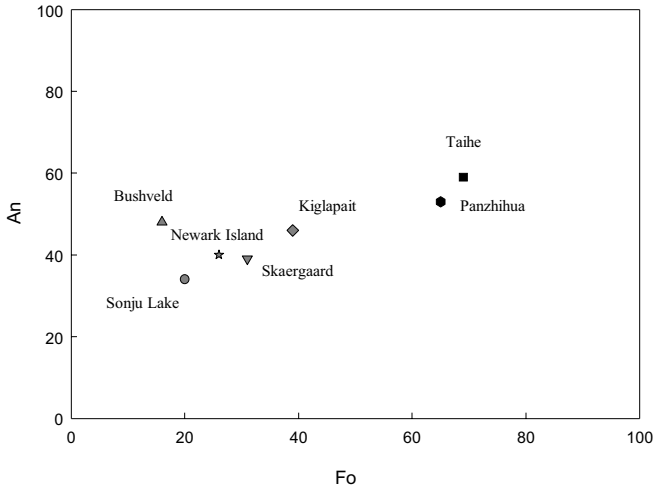
100
80
60
40
20
0
An
0
20
40
60
80
100
Fo
Taihe
Panzhihua
Kiglapait
Bushveld
Newark Island
Skaergaard
Sonju Lake

Fig. 2

This is a preprint, the final version is subject to change, of the American Mineralogist (MSA)
Cite as Authors (Year) Title. American Mineralogist, in press.
(DOI will not work until issue is live.) DOI: http://dx.doi.org/10.2138/am-2016-5577

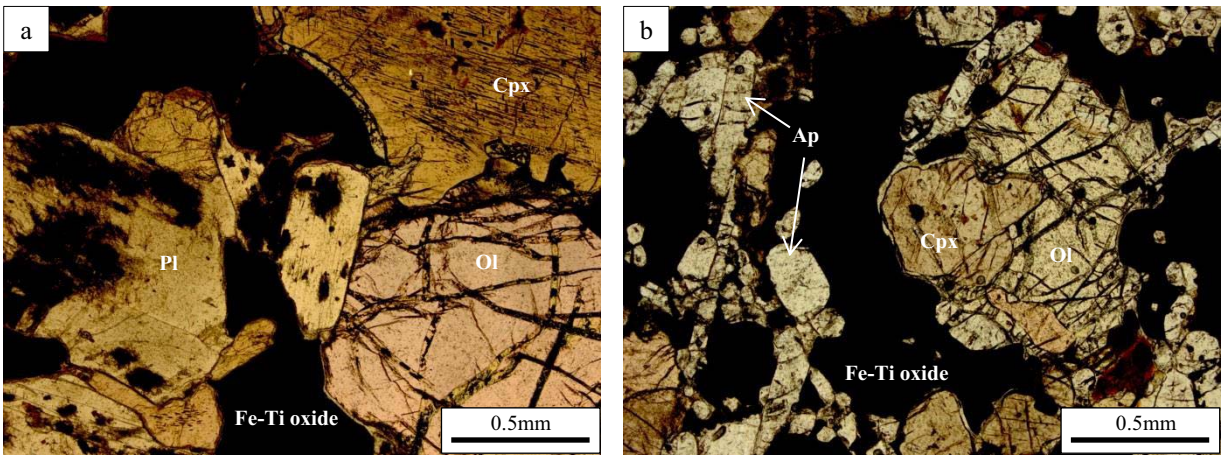

Fig. 3

This is a preprint, the final version is subject to change, of the American Mineralogist (MSA)
Cite as Authors (Year) Title. American Mineralogist, in press.
(DOI will not work until issue is live.) DOI: http://dx.doi.org/10.2138/am-2016-5577

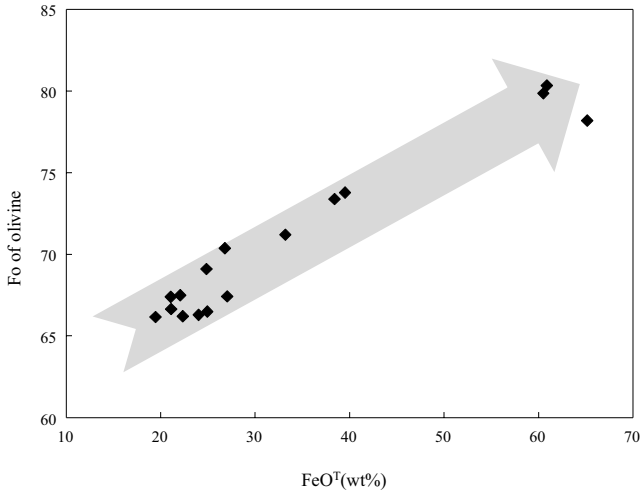

Fig. 4

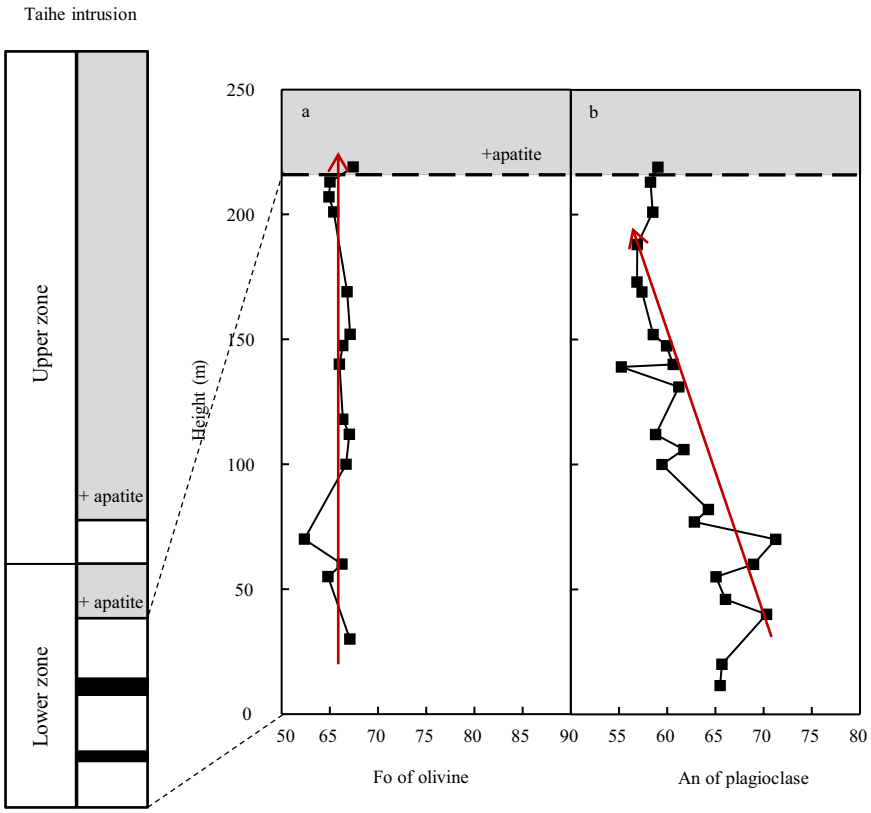
Taihe intrusion
Upper zone
Lower zone
+ apatite
+ apatite
Height (m)
250
200
150
100
50
0
a
b
+apatite
50 65 70 75 80 85 90
55 60 65 70 75 80
Fo of olivine
An of plagioclase

Fig. 5

This is a preprint, the final version is subject to change, of the American Mineralogist (MSA)
Cite as Authors (Year) Title. American Mineralogist, in press.
(DOI will not work until issue is live.) DOI: http://dx.doi.org/10.2138/am-2016-5577

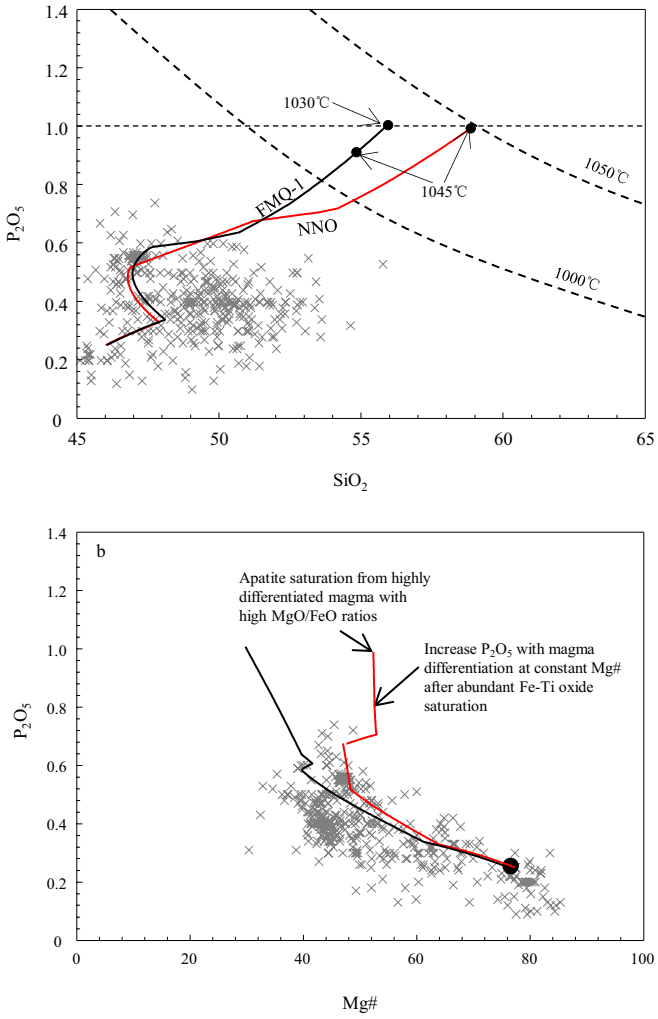

Fig. 6

Table 1: Compositions of olivine and plagioclase at the saturation of apatite in the mafic-ultramafic intrusions of the Emeishan large igneous province and other common layered intrusions

Phases	Taihe	Hongge[1]	Panzhihua[2]	Bushveld[3]	Skaergaard[4]	Kiglapait[5]	Sonju Lake, Duluth[6]	Newark Island[7]
Olivine (Fo)	69	72	65	16	31	39	20	26
Plagioclase (An)	59	-	53	48	39	46	34	40

Data sources: [1]Bai et al., (2012); [2]Pang et al., (2009); [3]Tegner et al., (2006); [4]McBirney, (1996); [5]Morse, (1979); [6]Park al., (2004); [7]Wiebe and Snyder, (1993).

This is a preprint, the final version is subject to change, of the American Mineralogist (MSA)
Cite as Authors (Year) Title. American Mineralogist, in press.
(DOI will not work until issue is live.) DOI: http://dx.doi.org/10.2138/am-2016-5577

Table 2. Average compositions of plagioclase from the Lower zone of the Taihe intrusion

Sample	ZK513-1	ZK513-3	ZK513-8	ZK513-9	ZK513-12	ZK513-15	ZK513-17	ZK513-18	ZK513-21	ZK513-24	ZK513-26	ZK513-28
Depth (m)	1389	1380	1360	1354	1345	1340	1330	1323	1318	1300	1294	1288
SiO_2	51.73	52.08	51.62	52.23	51.79	51.14	51.25	53.86	52.90	54.41	54.22	53.97
TiO_2	0.08	0.08	0.10	0.06	0.08	0.07	0.05	0.11	0.10	0.09	0.09	0.10
Al_2O_3	30.19	30.16	30.69	29.56	29.46	29.82	31.16	29.52	29.15	29.24	28.99	28.83
CaO	13.73	13.66	14.57	13.42	13.45	14.07	14.66	12.98	13.04	12.58	12.50	12.23
FeO	0.34	0.31	0.32	0.22	0.21	0.28	0.10	0.28	0.23	0.14	0.25	0.27
Na_2O	3.91	3.85	3.34	3.77	3.93	3.44	3.26	4.19	3.96	4.70	4.20	4.68
K_2O	0.14	0.14	0.10	0.08	0.10	0.10	0.01	0.08	0.08	0.07	0.12	0.09
Total	100.11	100.29	100.74	99.34	99.01	98.92	100.49	101.02	99.45	101.23	100.37	100.17
Si	2.36	2.37	2.34	2.39	2.38	2.36	2.32	2.42	2.41	2.44	2.44	2.44
Ti	0.00	0.00	0.00	0.00	0.00	0.00	0.00	0.00	0.00	0.00	0.00	0.00
Al	1.62	1.61	1.64	1.59	1.60	1.62	1.66	1.56	1.57	1.54	1.54	1.54
Ca	0.66	0.66	0.70	0.65	0.65	0.69	0.70	0.62	0.63	0.60	0.60	0.59
Fe	0.01	0.01	0.01	0.01	0.01	0.01	0.00	0.01	0.01	0.01	0.01	0.01
Na	0.34	0.34	0.29	0.33	0.35	0.31	0.29	0.36	0.35	0.41	0.37	0.41
K	0.01	0.01	0.01	0.00	0.01	0.01	0.00	0.00	0.00	0.00	0.01	0.01
Total	5.01	5.00	4.99	4.98	5.00	4.99	4.99	4.98	4.98	5.00	4.97	4.99
An	65.20	65.37	70.03	65.74	64.76	68.67	70.98	62.52	63.97	59.14	61.42	58.48

This is a preprint, the final version is subject to change, of the American Mineralogist (MSA)
Cite as Authors (Year) Title. American Mineralogist, in press.
(DOI will not work until issue is live.) DOI: http://dx.doi.org/10.2138/am-2016-5577

Continued

Sample	ZK513-30	ZK513-31	ZK513-32	ZK513-34	ZK513-36	ZK513-38	ZK513-39	ZK513-40	ZK513-42	ZK513-44	ZK513-45
Depth (m)	1269	1261	1260	1253	1248	1231	1227	1212	1199	1187	1181
SiO_2	52.99	56.13	54.85	54.28	54.85	55.40	54.78	54.74	55.08	54.65	54.71
TiO_2	0.11	0.07	0.11	0.10	0.12	0.09	0.09	0.08	0.10	0.10	0.13
Al_2O_3	28.27	28.34	29.33	28.86	28.76	28.62	28.44	28.56	28.58	28.45	28.59
CaO	12.38	11.65	12.47	12.27	12.24	12.03	11.98	11.99	12.05	11.98	12.10
FeO	0.29	0.08	0.29	0.14	0.29	0.28	0.24	0.29	0.30	0.30	0.30
Na_2O	4.23	5.20	4.46	4.51	4.68	4.79	4.90	4.89	4.54	4.60	4.50
K_2O	0.17	0.03	0.03	0.04	0.17	0.23	0.19	0.20	0.28	0.22	0.21
Total	98.44	101.49	101.54	100.19	101.11	101.43	100.62	100.74	100.93	100.30	100.54
Si	2.44	2.50	2.44	2.45	2.46	2.47	2.47	2.46	2.47	2.47	2.46
Ti	0.00	0.00	0.00	0.00	0.00	0.00	0.00	0.00	0.00	0.00	0.00
Al	1.53	1.48	1.54	1.54	1.52	1.50	1.51	1.51	1.51	1.51	1.52
Ca	0.60	0.55	0.59	0.59	0.58	0.57	0.57	0.57	0.57	0.57	0.58
Fe	0.01	0.00	0.01	0.01	0.01	0.01	0.01	0.01	0.01	0.01	0.01
Na	0.38	0.45	0.39	0.39	0.41	0.41	0.43	0.43	0.39	0.40	0.39
K	0.01	0.00	0.00	0.00	0.01	0.01	0.01	0.01	0.02	0.01	0.01
Total	4.98	4.98	4.98	4.98	4.99	4.99	5.00	5.00	4.98	4.98	4.98
An	60.90	54.91	60.30	59.61	58.22	57.06	56.54	56.58	58.17	57.96	58.71

This is a preprint, the final version is subject to change, of the American Mineralogist (MSA)
Cite as Authors (Year) Title. American Mineralogist, in press.
(DOI will not work until issue is live.) DOI: http://dx.doi.org/10.2138/am-2016-5577

Table 3. Average compositions of olivine from the lower zone of the Taihe intrusion

Sample	ZK13-5	ZK13-12	ZK13-15	ZK13-17	ZK13-24	ZK13-28	ZK13-29	ZK13-32	ZK13-34	ZK13-36	ZK13-38	ZK13-42	ZK13-43	ZK13-44	ZK13-45
Depth (m)	1370	1345	1340	1330	1300	1288	1282	1260	1253	1248	1231	1199	1193	1187	1181
Olivine composition (wt.%)															
SiO_2	39.23	37.88	37.73	39.94	38.68	37.82	37.12	40.27	39.70	38.71	38.23	37.61	37.82	37.87	38.23
TiO_2	0.01	0.03	0.02	0.01	0.03	0.02	0.02	0.04	0.03	0.02	0.03	0.02	0.04	0.02	0.02
MgO	36.32	32.12	32.02	39.91	35.33	33.06	32.12	40.98	41.04	36.78	33.41	31.93	32.76	33.21	34.05
CaO	0.08	0.09	0.06	0.09	0.08	0.04	0.05	0.12	0.07	0.07	0.05	0.05	0.05	0.08	0.07
MnO	0.50	0.50	0.54	0.31	0.44	0.52	0.57	0.36	0.34	0.41	0.67	0.64	0.70	0.62	0.60
FeO	23.48	28.85	28.56	20.29	25.47	28.51	29.29	18.42	17.91	23.29	28.68	29.05	29.98	28.60	27.14
NiO	0.02	0.04	0.03	0.03	0.02	0.01	0.02	0.01	0.01	0.01	0.00	0.01	0.00	0.01	0.00
Na_2O	0.01	0.03	0.05	0.01	0.02	0.02	0.07	0.02	0.03	0.01	0.01	0.04	0.01	0.04	0.02
Total	99.64	99.54	99.00	100.60	100.08	99.99	99.25	100.21	99.12	99.29	101.08	99.35	101.36	100.45	100.13
Si	1.03	1.02	1.02	1.02	1.02	1.01	1.01	1.02	1.02	1.02	1.01	1.02	1.01	1.01	1.02
Ti	0.00	0.00	0.00	0.00	0.00	0.00	0.00	0.00	0.00	0.00	0.00	0.00	0.00	0.00	0.00
Mg	1.42	1.29	1.29	1.52	1.39	1.32	1.30	1.55	1.57	1.44	1.32	1.29	1.30	1.32	1.35
Ca	0.00	0.00	0.00	0.00	0.00	0.00	0.00	0.00	0.00	0.00	0.00	0.00	0.00	0.00	0.00
Mn	0.01	0.01	0.01	0.01	0.01	0.01	0.01	0.01	0.01	0.01	0.02	0.01	0.02	0.01	0.01
Fe^{2+}	0.51	0.65	0.65	0.43	0.56	0.64	0.67	0.39	0.38	0.51	0.64	0.66	0.67	0.64	0.60
Ni	0.00	0.00	0.00	0.00	0.00	0.00	0.00	0.00	0.00	0.00	0.00	0.00	0.00	0.00	0.00
Na	0.00	0.00	0.00	0.00	0.00	0.00	0.00	0.00	0.00	0.00	0.00	0.00	0.00	0.00	0.00
Total	2.97	2.98	2.98	2.98	2.98	2.99	2.99	2.98	2.98	2.98	2.99	2.98	2.99	2.99	2.98
Fo	73.4	66.5	66.7	77.8	71.2	67.4	66.2	79.9	80.3	73.8	67.5	66.2	66.1	67.4	69.1
Fo_{Fe20}^*	67.1	64.8	66.3	62.4	66.7	67.0	66.3	66.0	66.3	67.1	66.8	65.4	64.7	65.0	67.4

*Fo_{Fe20}: The primary Fo before subsolidus Fe-Mg exchange reaction between olivine and Fe-Ti oxides, Calculated at whole-rock FeO^T=20 wt.%